Photobiomodulation provides neuroprotection through regulating mitochondrial fission imbalance in the subacute phase of spinal cord injury

Xin Li[1, 2, #], Xuan-Kang Wang[1, #], Zhi-Jie Zhu[1, #], Zhuo-Wen Liang[1], Peng-Hui Li[1], Yang-Guang Ma[1], Tan Ding[1], Kun Li[1], Xiao-Shuang Zuo[1], Cheng Ju[1], Zhi-Hao Zhang[1], Zhi-Wen Song[1], Hui-Lin Quan[1], Jia-Wei Zhang[1], Liang Luo[1], Zhe Wang[1, *], Xue-Yu Hu[1, *]

https://doi.org/10.4103/1673-5374.366491

Date of submission: June 3, 2022

Date of decision: August 16, 2022

Date of acceptance: November 21, 2022

Date of web publication: January 5, 2023

From the Contents

Graphical Abstract

Photobiomodulation prevents neuronal death by restoring mitochondrial fragmentation in neurons following spinal cord injury

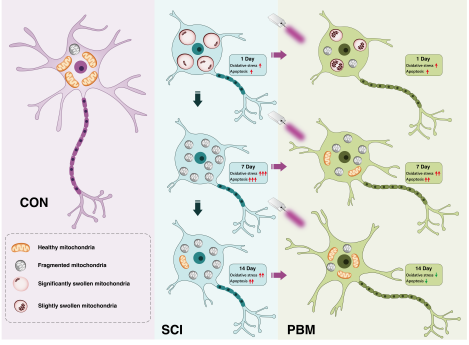

Abstract

Increasing evidence indicates that mitochondrial fission imbalance plays an important role in delayed neuronal cell death. Our previous study found that photobiomodulation improved the motor function of rats with spinal cord injury. However, the precise mechanism remains unclear. To investigate the effect of photobiomodulation on mitochondrial fission imbalance after spinal cord injury, in this study, we treated rat models of spinal cord injury with 60-minute photobiomodulation (810 nm, 150 mW) every day for 14 consecutive days. Transmission electron microscopy results confirmed the swollen and fragmented alterations of mitochondrial morphology in neurons in acute (1 day) and subacute (7 and 14 days) phases. Photobiomodulation alleviated mitochondrial fission imbalance in spinal cord tissue in the subacute phase, reduced neuronal cell death, and improved rat posterior limb motor function in a time-dependent manner. These findings suggest that photobiomodulation targets neuronal mitochondria, alleviates mitochondrial fission imbalance-induced neuronal apoptosis, and thereby promotes the motor function recovery of rats with spinal cord injury.

Key Words: low-level laser therapy; mitochondria; mitochondrial dynamics; mitochondrial fission imbalance; neuron; photobiomodulation; secondary injury; spinal cord injury

Introduction

Spinal cord injury (SCI), resulting from sudden or sustained trauma, can result in neurological cell death that contributes to long-term disability and sensory deficits (Jazayeri et al., 2015; Hachem et al., 2017; Donovan and Kirshblum, 2018). Mechanistically, the majority of neuronal cell death originates from a phase of delayed secondary injury with progressive cascades, such as oxidative stress (Fatima et al., 2015), inflammation (Qiao et al., 2010, 2015) and mitochondrial disruption (Fatima et al., 2015; Scholpa and Schnellmann, 2017), rather than from the primary injury, referring to the immediate mechanical trauma.

Mitochondria modulate free radical formation, buffer calcium, and generate energy, and thereby affect immune response, autophagy and cell survival (Grohm et al., 2012; Tait and Green, 2012; Gollihue and Rabchevsky, 2017; Ozgen et al., 2022; Rey et al., 2022). Among the mechanisms of secondary injury progressive cascades, mitochondrial disruptions, including morphological alterations, mitophagy, adenosine triphosphate (ATP) loss, mitochondrial-mediated apoptosis and mitochondrial oxidative stress, play a particularly critical role in neuronal death cascades in neurodegenerative diseases and central nervous system injuries (Calkins et al., 2011; Liu et al., 2016; Suárez-Rivero et al., 2016; Ottolini et al., 2017; Chen et al., 2018; Zhang et al., 2021). Restoration of mitochondrial disruptions has been shown to be a potentially effective therapeutic strategy for secondary injury after SCI, with strategies including mitochondrial permeability transition pore inhibitors (McEwen et al., 2007; Ravikumar et al., 2007), biofuels (Ravikumar et al., 2007; Patel et al., 2010), antioxidants (Hall, 2011; Bains and Hall, 2012; Chen et al., 2018) and mitochondrial division inhibitors (Li et al., 2015; Liu et al., 2015).

Mitochondria exist in dynamic networks that continuously undergo fusion and fission. The number and morphology of mitochondria within cells are closely related to mitochondrial function. Under pathological conditions, mitochondria morphology and number vary with the demand for mitochondrial homeostasis (Hoppins et al., 2007; Youle and van der Bliek, 2012; Meyer et al., 2017). Research in the past decade has shown that an imbalance of mitochondrial dynamics, which shifts the balance toward fission, may produce an accumulation of mitochondrial DNA defects, ATP depletion, and impaired regulation of oxidative stress, thereby promoting neuronal death (Grohm et al., 2010, 2012; Lu et al., 2017). These studies suggested that during neuronal cell death, dynamic tubulation of mitochondria was fragmented into smaller and dysfunctional organelles. However, it remains unknown whether mitochondrial fission imbalance regulates neuronal cell death in subacute SCI. If so, as reported in previous studies (Grohm et al., 2012; Li et al., 2015; Liu et al., 2015), restoration of mitochondrial dynamics might be an effective therapeutic strategy to ameliorate delayed neuronal cell death.

[1]Department of Orthopedics, Xijing Hospital, Fourth Military Medical University, Xi'an, Shaanxi Province, China; [2]967 Hospital of People's Liberation Army Joint Logistic Support Force, Dalian, Liaoning Province, China

*Correspondence to: Xue-Yu Hu, MD, huxueyu@fmmu.edu.cn; Zhe Wang, MD, wangzhe@fmmu.edu.cn.

https://orcid.org/0000-0003-0852-1196 (Xue-Yu Hu); https://orcid.org/0000-0002-7573-1583 (Zhe Wang)

#These authors contributed equally to this work.

Funding: *This study was supported by the National Natural Science Foundation of China, Nos. 81070996 (to ZW) and 81572151 (to XYH); and Shaanxi Provincial Key R&D Program, Nos. 2020ZDLSF02-05 (to ZW), 2021ZDLSF02-10 (to XYH).*

How to cite this article: *Li X, Wang XK, Zhu ZJ, Liang ZW, Li PH, Ma YG, Ding T, Li K, Zuo XS, Ju C, Zhang ZH, Song ZW, Quan HL, Zhang JW, Luo L, Wang Z, Hu XY (2023) Photobiomodulation provides neuroprotection through regulating mitochondrial fission imbalance in the subacute phase of spinal cord injury. Neural Regen Res 18(9):2005-2010.*

In recent years, medical application of low-energy lasers with light in the red to near-infrared range (630–1000 nm) has become known as low-level laser therapy or photobiomodulation (PBM), and its use has broadened to central nervous system diseases and injuries (Ying et al., 2008; Huisa et al., 2013; Xuan et al., 2014; Micheli et al., 2017, 2019). There is growing evidence indicating that PBM, especially the wavelength of 810 nm, acts on cells through a primary photoacceptor, which has been identified as cytochrome C oxidase, part of mitochondrial complex IV, to convert light energy into chemical energy. Activation of cytochrome C oxidase then initiates related changes in mitochondria and downstream expression of many protective gene products with anti-apoptotic, anti-oxidant, and pro-proliferation effects (Karu et al., 1994, 2003, 2004, 2005; Morimoto et al., 1994; Pastore et al., 2000; Eells et al., 2004; Liang et al., 2006; Yeager et al., 2006; Karu, 2008). In a beta amyloid-induced Alzheimer's disease rat model, PBM ameliorated mitochondrial fragmentations to reduce oxidative stress and neuronal damage (Lu et al., 2017). Mitochondria might evolve from photosynthetic organisms (Cavalier-Smith, 2006), and a low-energy laser was shown to increase ATP production and mitochondrial DNA replication (Vacca et al., 1993). Thus, it can be hypothesized that an 810 nm laser may improve the mitochondrial response to SCI to enhance the therapeutic effects.

On the basis of the above studies, we postulated that impaired modulation of mitochondrial dynamics toward fission during secondary injury results in delayed neuronal cell death in SCI rats, and that PBM might have a positive effect on neural protection. In the present study, transmission electron microscopy (TEM) was used to detect mitochondrial morphology in neurons after SCI. We also investigated the effects of PBM on self-repair of mitochondrial fragmentation and neuronal cell death *in vivo*. This study is the first to examine whether PBM has a therapeutic effect for SCI via ameliorating mitochondrial fission imbalance in the subacute phase of SCI.

Methods

Crush injury model in rat and laser treatment

This research project was approved by the Welfare and Ethics Committee of Experimental Animal Center of Fourth Military Medical University (approval No. 20210452) on April 1, 2021. All experiments were designed and reported according to the Animal Research: Reporting of *In Vivo* Experiments (ARRIVE) guidelines (Percie du Sert et al., 2020).

Adult male Sprague-Dawley rats (8 weeks old and weighing 250–280 g) were purchased from Experimental Animal Center of Fourth Military Medical University (license No. SYXK (Shaan) 2019-001). A total of 162 rats were randomly divided into Sham, SCI, and PBM treatment groups (**Additional Figure 1**).

The SCI model was established with the bilateral spinal cord compression method, as performed in a previous study (Song et al., 2017) with some modifications. Rats were anesthetized with an intraperitoneal injection of 1% pentobarbital (50 mg/kg, Huimei Biotechnology Co., Ltd, Xi'an, Shaanxi Province, China). Then, a midline dorsal thoracic incision was made above the T8–T12 vertebrae to expose the vertebral column. A laminectomy was performed with rongeurs at the T11 level, exposing the spinal cord. Forceps with metal spacers were used to laterally compress the spinal cord to a fixed thickness of 0.5 mm, and the compression was held for 40 seconds. Both hind limbs twitching involuntarily and the tail twisting indicated the successful completion of the SCI model.

In the PBM treatment rats, the head and tail of the light-emitting area of the optical fiber (Yazetech Medical Technology Co., Ltd, Xi'an, Shaanxi Province, China) were sutured to the paravertebral soft tissues of the T10 and T12 vertebrae after SCI, respectively. Immediately after SCI, 810-nm infrared light with an average radiant power of 150 mW (Lei Shi Optoelectronics Co., Ltd, Changchun, Jilin Province, China) was used for the treatment, 60 minutes each time, once a day. In the sham operation animals, the T8–T12 spinal cord received the identical surgical procedure but with no crush injury or laser irradiation; these were regarded as the control groups. After operation, an intramuscular injection of penicillin G (70 mg/kg) was administered to protect the rats from infection once per day for 7 days, and manual bladder expression was performed twice per day until the animals regained bladder function. The rats were sacrificed 12 hours after PBM treatment for subsequent analyses. SCI was divided into acute (at 1 day after SCI) and subacute stages (at 7 and 14 days after SCI) according to the duration of the injury. The detailed animal experimental design for the study was illustrated in **Additional Figure 1**.

Transmission electron microscopy

To detect mitochondrial morphology and number in neurons, spinal cord sample preparations were conducted for TEM at 1, 7 and 14 days after SCI. Rats were sacrificed after anesthesia as described above and perfused with 4% glutaraldehyde. The tissue centered on the injured area was cut perpendicular to the long axis into blocks 2 mm wide and postfixed with 4% glutaraldehyde overnight. The tissue was then fixed with 2.5% glutaraldehyde for 2 hours, postfixed with 2% osmium tetroxide, dehydrated with a graded ethanol series, embedded in resin, sliced with an ultramicrotome (Leica, Wetzlar, Germany), stained and viewed on a Tecnai G2 TEM (Thermo Fisher, Waltham, MA, USA) at 80 kV. Elongated mitochondria were defined as mitochondria with a ratio between the major and minor axis greater than 2 (Calkins et al., 2011). Mitochondrial area was defined as the cross-sectional area. Feret's diameter was calculated as longest distance between any two points of the mitochondrial external perimeter. Mitochondrial area, diameter and number were measured by FIJI analysis software (Fiji-64bit, National Institutes of Health, Bethesda, MD, USA; Schindelin et al., 2012).

Western blot analysis

Mitochondrial fractions were prepared using a kit (C3606, Beyotime Institute of Biotechnology, Nantong, Jiangsu Province, China). Rats were deeply anesthetized and sacrificed at 7 and 14 days postoperation, and a 0.5-cm segment of spinal cord centered on the injury site was rapidly stripped. Fresh tissue was homogenized in ice-cold mitochondria isolation reagent A containing 1 mM phenylmethylsulfonyl fluoride and centrifuged at 600 × *g* for 10 minutes at 4°C. The supernatants were transferred to another tube and centrifuged at 11 000 × *g*, 4°C for 10 minutes to precipitate the mitochondria. The isolated mitochondria were digested by cold mitochondrial lysis buffer and then subjected to western blotting analysis.

The mitochondrial proteins (10 μg) were loaded onto 4–20% Bis-Tris gels (M00656, GenScript, Nanjing, Jiangsu Province, China), transferred onto a nitrocellulose membrane (EMD Millipore Corp, Burlington, MA, USA), blocked and then incubated with primary antibody to mitochondrial fission 1 (Fis1; rabbit, 1:1000, Proteintech Group, Wuhan, Hubei Province, China, Cat# 10956-1-AP, RRID: AB_2102532), mitochondrial fission factor (Mff; rabbit, 1:1000, Proteintech Group, Cat# 17090-1-AP, RRID: AB_2142463), dynamin-related protein 1 (Drp1; rabbit, 1:2000, Cell Signaling Technology, Danvers, MA, USA, Cat# 8570S, RRID: AB_10950498), or heat shock protein 60 (rabbit, 1:3000, Servicebio, Wuhan, Hubei Province, China, Cat# GB11243) overnight at 4°C in blocking buffer. After incubation with goat anti-rabbit horseradish peroxidase antibody (1:1000, InCellGene, San Antonio, TX, USA, Cat# SA-10011 or goat anti-mouse horseradish peroxidase antibody (1:1000, InCellGene, Cat# SA-10010) at 25°C for 1 hour, visualization was detected by chemiluminescence (Amersham Imager 600, General Electric, Boston, MA, USA). Optical density was performed using FIJI analysis software.

Malondialdehyde, 3-nitrotyrosine, superoxide dismutase and total antioxidant capacity assay

Oxidative stress and antioxidative parameters were measured from spinal cord homogenates at 1, 7 and 14 days after SCI. Lipid Peroxidation MDA Assay Kit (Cat# S0131M, Beyotime Institute of Biotechnology) and Nitrotyrosine ELISA Kit (Cat# MM-70408R1, Jiangsu Meimian Industrial Co., Ltd, Suining, Jiangsu Province, China) were used to measure oxidative stress markers specific to lipid oxidation (malondialdehyde, MDA) and protein oxidation (3-nitrotyrosine, 3-NT), respectively. Superoxide Dismutase Assay Kit (Cat# S0101M, Beyotime Institute of Biotechnology) and Total Antioxidant Capacity Assay Kit (Cat# S0116, Beyotime Institute of Biotechnology) were used to measure antioxidative parameters superoxide dismutase (SOD) and total antioxidant capacity (TAOC), respectively. The detailed experimental manipulations were performed according to the manufacturer's instructions. The absorbances were detected using a microplate reader (SYNERGY H1, BioTek, Winooski, VT, USA) at 532, 450, 450, and 593 nm for MDA, 3-NT, SOD and TAOC, respectively.

Immunofluorescence staining

Rats were deeply anesthetized as described above and sacrificed for collection of frozen sections in gray matter of the injured spinal cord, according our previous method (Wang et al., 2021). Approximately 10-μm-thick serial sagittal sections were sliced and then placed on slides. Frozen sections from rats at 1, 7 and 14 days post-SCI were washed three times with phosphate buffer saline, permeabilized with 1% Triton X-100, and blocked with 5% bovine serum albumin and normal goat serum for 1 hour at 25°C. After blocking, sections were incubated with primary antibody of microtubule-associated protein 2 (MAP2; rabbit, 1:200, Cell Signaling Technology, Cat# 8707T, RRID: AB_2722660) at 4°C overnight, which is a sensitive indicator for the assessment of neuronal injury. The sections were then incubated with secondary antibody (Cy3-conjugated donkey anti-rabbit IgG, 1:200, Jackson Immuno Research, West Grove, PA, USA, Cat# 159918, RRID: AB_2307443) for 1 hour at 25°C at room temperature and stained with the 4′,6-diamidino-2-phenylindole (C0065, Solarbio, Beijing, China) to detect the nucleus. Immunostaining images of MAP2 dispersion were observed with confocal microscopy (FV3000, Olympus Corporation, Tokyo, Japan), and dispersion was calculated as the area of pore unstained with MAP2 or 4′,6-diamidino-2-phenylindole divided by the total area.

TdT-mediated dUTP nick end labeling staining

To assess the level of spinal cord tissue apoptosis at 14 days post-SCI, the one step TdT-mediated dUTP nick end labeling (TUNEL) apoptosis assay kit (Cat# C1090, Beyotime Institute of Biotechnology) was used, according to our previous method (Wang et al., 2021). Fragmented DNA of apoptotic cells was stained red by TUNEL, and images were obtained from a fluorescence microscope (Olympus Corporation, BX51).

Basso, Beattie, and Bresnahan score and footprint analysis

After SCI, the Basso, Beattie, and Bresnahan (BBB) locomotor scale (Basso et al., 1995) was used to assess behavioral function every day until rats were sacrificed. The observers were blind to experimental groups and familiar with the scoring criteria. BBB is a 22-point scale that indicates hindlimb functional recovery, where a score of 0 indicates complete paralysis and a score of 21 indicates normal walking.

Footprint analysis was performed to assess motor coordination at 14 days post-surgery, as described in a previous study (de Medinaceli et al., 1982).

The back and feet of the hindlimbs were stained with red ink and blue ink, respectively. Stride length and stride width of the footprints were obtained from papers covering a narrow runway of 1 m length and 7 cm width. Stride length was determined as the distance between the central pads of two consecutive prints and stride width was measured as the distance between the central pads of the hindpaws.

Statistical analysis

The differences in BBB scores were evaluated by Scheirer-Ray-Hare test in SPSS 25.0 (IBM Corp., Armonk, NY, USA) (Guan et al., 2021). GraphPad Prism 7.00 (GraphPad Software, San Diego, CA, USA, www.graphpad.com) was used to carry out other statistical analyses. One-way analysis of variance with least significant difference *post hoc* analysis was used for multiple comparisons. For all analyses, the significance of statistical analyses was set at a level of 0.05. All data are presented as mean ± standard error of the mean (SEM).

Results

PBM enhances the self-repair of mitochondrial dynamics *in vivo*

To explore the effects of PBM on the dynamic tubulation of mitochondria, TEM was used to examine mitochondrial morphology in individual neurons from rats at 1, 7 and 14 days postsurgery (**Figure 1**). Representative TEM images showed that mitochondria were present in dynamic networks in control rats (**Figure 1A**). At 1 day, mitochondrial alterations in the neurons from SCI rats were characterized by decreased mitochondrial number, increased mitochondrial area and cristae loss, and the percentage of swollen mitochondria in SCI rats was higher than that in the control animals. Treatment with PBM restored the alterations in mitochondrial number, mitochondrial volume, cristae loss and the percentage of swollen mitochondria to some extent, though the measures did not reach the levels of the control group (**Figure 1A–E** and **Additional Figure 2**). At 7 and 14 days, the absolute number of mitochondria per neuron in SCI rats was significantly higher than that in control rats, and the majority of mitochondria exhibited short and round appearance (**Figure 1A**, **F** and **G**). PBM treatment attenuated the decrease in the percentage of elongated mitochondria (**Figure 1F**) and the increase in mitochondria number (**Figure 1G**) at 7 and 14 days. Interestingly, SCI rats at 14 days post-surgery had a higher percentage of elongated mitochondria (**Figure 1F**) and a lower number of mitochondria (**Figure 1G**) than those at 7 days, and PBM treatment for 14 consecutive days had a larger effect than treatment for 7 consecutive days (**Figure 1F** and **G**). Data of the PBM treatment groups did not reach the control group levels except for mitochondria number at 14 days post-surgery (**Figure 1F** and **G**).

PBM enhances the self-repair of mitochondrial targeting fission proteins *in vivo*

We next investigated the effects of PBM on mitochondrial targeting fission proteins after SCI. Western blot analysis showed that the expression levels of fission-related proteins (Drp1, Fis1 and Mff) in the SCI rats were higher than those in the control rats at 7 (**Figure 2A**) and 14 days (**Figure 2B**) after SCI, and administration of PBM decreased the expression levels of fission-related proteins compared with those from SCI rats at 7 and 14 days. The expression levels of fission-related proteins in the PBM rats were higher than those in the control rats at 7 days, except for Fis1 protein (**Figure 2A**). There were no significant differences in the fission-related protein expression levels between the control and PBM groups at 14 days, except for Mff protein (**Figure 2B**). In addition, the SCI rats at 14 days had lower levels of fission-related proteins than those at 7 days (**Figure 2C**), and the SCI rats with PBM for 14 consecutive days showed lower levels of fission-related proteins than those for 7 consecutive days, except for Fis1 protein (**Figure 2D**), indicating that PBM enhanced the self-repair of mitochondrial targeting fission proteins in a time-dependent manner.

PBM enhances the self-repair of mitochondrial oxidative stress *in vivo*

To explore the effects of PBM on oxidative stress, oxidative stress markers specific to protein and lipid oxidation, 3-NT and MDA, and anti-oxidant parameters, SOD and TAOC, were detected in spinal cord tissue homogenates at 1, 7 and 14 days postsurgery. In the acute phase (1 day postsurgery), the SCI group had a marked increase in 3-NT level, but not MDA level compared with the control group (**Figure 3A** and **B**). Anti-oxidant markers were significantly reduced in SCI groups compared with control rats (**Figure 3C** and **D**). Compared with the SCI group at 1 day, the PBM treatment group had no significant difference in the levels of 3-NT, MDA and SOD (**Figure 3A–D**). At 7 days, SCI rats had the highest levels of oxidative stress markers (**Figure 3A** and **B**) and the lowest levels of anti-oxidant markers (**Figure 3C** and **D**). Interestingly, rats with PBM treatment at 7 days had higher levels of oxidative stress markers (**Figure 3A** and **B**) and lower levels of anti-oxidant markers (**Figure 3C** and **D**) than those at 1 day.

Similar to the trend of mitochondrial morphological alterations in the subacute phase, SCI rats at 7 and 14 days post-surgery had higher oxidative stress markers (**Figure 3A** and **B**) and lower anti-oxidant parameters (**Figure 3C** and **D**) than the controls, and PBM attenuated the increase of oxidative stress markers and the decrease of anti-oxidant parameters to some extent. The SCI rats with PBM for 14 consecutive days showed lower levels of oxidative stress markers (**Figure 3A** and **B**) and higher levels of anti-oxidant parameters (**Figure 3C** and **D**) than those with PBM for 7 consecutive days, suggesting that longer PBM treatment had a greater effect on self-repair of oxidative stress.

PBM improves neuronal damage and locomotor function after SCI

To assess the impact of PBM on neuronal injury, MAP2 dispersion was examined to assess the degree of neuronal injury. Confocal fluorescence images indicated that the neurons in the gray matter of the normal ventral spinal cord were tightly arranged with low MAP2 dispersion (**Figure 4A–C**). SCI significantly increased MAP2 dispersion at 1 (**Figure 4A**), 7 (**Figure 4B**) and 14 (**Figure 4C**) days after injury. SCI rats at 7 days had a higher level of MAP2 dispersion than those at 1 day (**Figure 4D**). PBM did not improve MAP2 dispersion at 1 day (**Figure 4A**), and PBM treatment for 7 and 14 consecutive days decreased MAP2 dispersion, but MAP2 dispersion did not reach the levels of the controls (**Figure 4D**). TUNEL staining confirmed that PBM improved apoptosis at 14 days after SCI (**Additional Figure 3**). Rats with PBM treatment at 7 days had a higher level of MAP2 dispersion compared with rats with PBM treatment at 1 day (**Figure 4D**). In addition, MAP2 dispersion was lower in the SCI rats at 14 days after operation than that at 7 days, suggesting self-repair of neuronal injury (**Figure 4D**). The neurons of ventral spinal cord around the injured area from rats with 14-day PBM had substantially lower MAP2 dispersion than those with 7-day PBM (**Figure 4D**).

BBB test and footprint analysis were performed for behavioral assessments of functional recovery. The highest BBB score of 21 was observed in the control group over the entire time range (**Figure 5A**), indicating that the sham surgical operation did not damage the spinal cord. Within the first 3 days after surgery, there was no significant difference in BBB score between the SCI and PBM groups. However, BBB score of PBM rats was higher than that of SCI rats from the 4th day after surgery, and the BBB score of the PBM group was rapidly restored from an average value of 5 to 11.6 on the 8th to 11th days, respectively, suggesting the therapeutic effect of PBM increased over time (**Figure 5A**). Finally, footprint analyses at 14 days after injury for the SCI group showed a reduction in stride lengths, an increase in stride widths and obvious instep dragging (**Figure 5B–D**). The PBM group showed a better restoration of stride length and stride width and clearer plantar stepping with less toe dragging compared with the SCI group, suggesting restoration of the base of support and motor function.

Discussion

Previous studies have elucidated that the number and morphology of mitochondria play an indispensable role in neuronal function and cell death, and have shown that restoration of mitochondrial fission imbalance is an effective therapeutic strategy for neuronal damage (Grohm et al., 2012; Li et al., 2015; Liu et al., 2015). Using a rat model of spinal cord crush injury, the present study was the first to explore the potential role and underlying mechanisms of PBM to alleviate mitochondrial dynamics defects in neurons after SCI.

Our data confirmed that mechanical damage resulted in a decrease in the number of mitochondria, swelling, and reduction or even disappearance of cristae in the acute phase after SCI. Mitochondrial alterations in the acute phase likely led to oxidative stress and rapid neuronal death. Our findings suggest that as injury progressed, mitochondrial dynamics transitioned to an imbalance of fission and contributed to worsened outcomes in oxidative stress and neuronal damage. Although PBM ameliorated mitochondrial changes in the acute phase to some extent, it did not improve oxidative stress and neuronal damage. Interestingly, the results suggest that PBM restored oxidative stress and neuronal damage by ameliorating the mitochondrial fission imbalance in the subacute phase in a time-dependent manner. Our findings provide evidence that PBM might be a promising therapeutic strategy for SCI.

Research in recent years has demonstrated that impaired mitochondrial fission balance is commonly observed after SCI (Cao et al., 2013; Li et al., 2015; Liu et al., 2015; Jia et al., 2016) and is intimately related to mitochondrial dysfunction resulting in neuronal death. Following SCI in rats, mitochondrial fragmentation was detected at 24 hours (Cao et al., 2013; Jia et al., 2016), and whether mitochondrial fragmentation persists long term has not yet been reported. Mitochondrial division inhibitor-1, a selective Drp1 inhibitor, blocked mitochondrial fragmentation to improve ATP generation, eliminate excessive reactive oxygen species, and contribute to functional neuroprotection (Li et al., 2015; Liu et al., 2015). PBM was demonstrated as an effective physical therapy to restore the imbalance of mitochondrial division (Lu et al., 2017). Our previous research showed that PBM with an *in vivo* optical fiber implantation may be safe and stable and could be used to directly project light onto the spinal cord surface (Liang et al., 2020).

In the present study, we found that the morphology and number of mitochondria in neurons varied with the prolonged injury time. Compared with the control group, the absolute number of mitochondria per area in SCI group was significantly lower and the majority of mitochondria in SCI group exhibited swollen appearance in acute phase of SCI. However, the absolute number of mitochondria per neuron was significantly higher in SCI group and the majority of mitochondria in SCI group were fragmented in the subacute phase of SCI, suggesting a crucial role of mitochondrial fission imbalance in the subacute phase. Delayed secondary injury usually begins within minutes to hours after SCI and can last for weeks to months, depending on the extent of the injury (Qiao et al., 2010, 2015; Scholpa and Schnellmann, 2017). Consistent with the mitochondrial changes that were observed, there were significant differences between SCI rats in the acute and subacute phases for mitochondrial oxidative stress and neuronal damage, suggesting that mitochondrial fission imbalance worsened outcomes in oxidative stress and neuronal damage of SCI rats in the subacute phase. Our results are the first to provide evidence that mitochondrial fission imbalance in the subacute phase worsens delayed secondary injury in SCI.

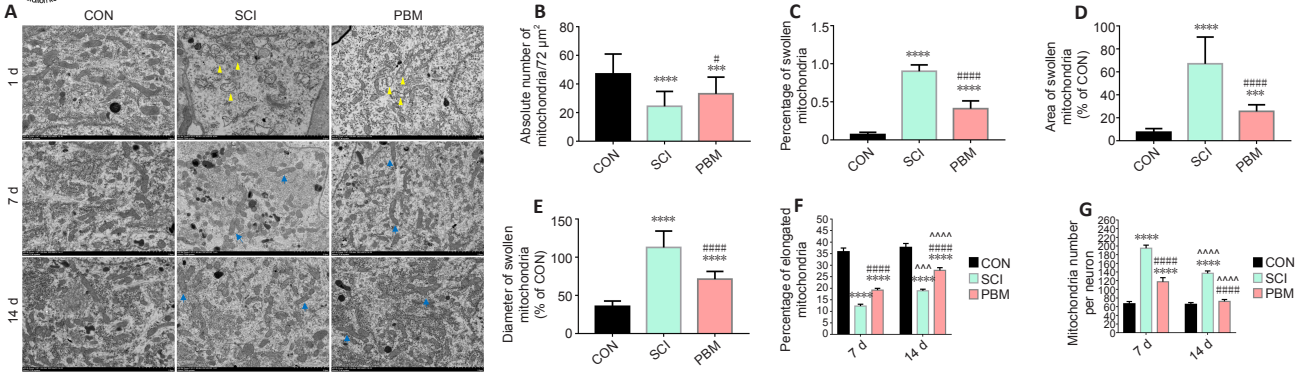

Figure 1 | **Effects of PBM on mitochondrial dynamics within neurons in spinal cord at 1, 7, and 14 days after SCI.**
(A) Representative TEM photographs of mitochondrial morphology. Mitochondria in neurons appeared swollen at 1 day after SCI and fragmented at 7 and 14 days. Fragmentation and swelling of mitochondria was improved to varying degrees by PBM. Data were collected from 20 photographs of five rats in each group. Yellow arrowheads point to swollen mitochondria and blue arrows point to elongated mitochondria. Scale bars: 2 μm. (B–E) Quantitative analyses of the absolute number of mitochondria (B), the percentage of swollen mitochondria (C), the area of swollen mitochondria (D), and the diameter of swollen mitochondria (E) at 1 day after SCI. (F, G) Quantitative analyses of the percentage of elongated mitochondria (F) and the absolute number of mitochondria per neuron (G). Data are expressed as mean ± SEM (n = 5). The values from the area and diameter of swollen mitochondria were calculated and expressed as percentage changes *versus* control group. ***P < 0.001, ****P < 0.0001, *vs.* CON group; #P < 0.05, ####P < 0.0001, *vs.* SCI group; ^^^P < 0.001, ^^^^P < 0.0001, *vs.* 7 days post-operation (one-way analysis of variance followed by least significant difference *post hoc* test). CON: Control; PBM: photobiomodulation; SCI: spinal cord injury; TEM: transmission electron microscope.

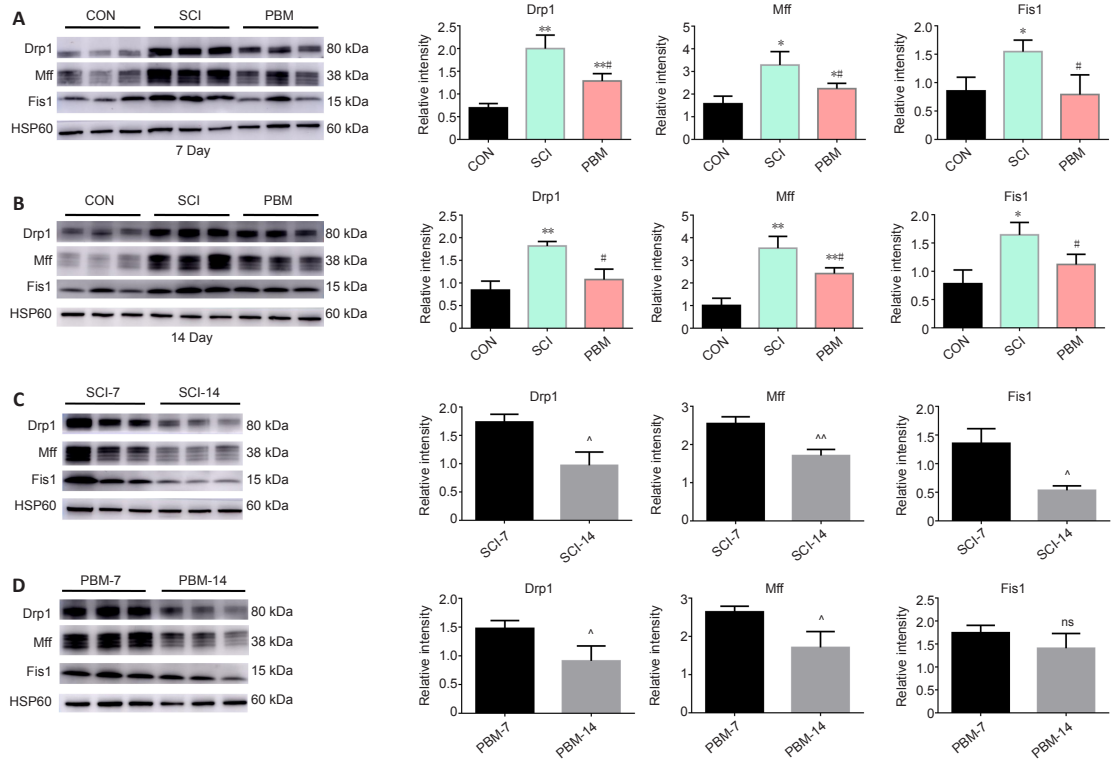

Figure 2 | **Effects of PBM on mitochondrial fission-related proteins at 7 and 14 days after SCI.**
(A, B) Representative western blot analyses and quantitative analyses of mitochondrial fractions for fission-related proteins Drp1, Fis1 and Mff at 7 (A) and 14 (B) days post-SCI. (C, D) Representative western blot analyses and quantitative analyses of Drp1, Fis1 and Mff to compare levels between SCI rats with or without PBM at 7 (C) and 14 (D) days post-SCI. HSP60 was used as a reference protein for mitochondrial proteins. Data are expressed as mean ± SEM (n = 3). *P < 0.05, **P < 0.01, *vs.* CON group; #P < 0.05, *vs.* SCI group; ^P < 0.05, ^^P < 0.01, *vs.* 7 days post-operation (one-way analysis of variance followed by least significant difference *post hoc* test). CON: Control; Drp1: dynamin-related protein 1; Fis1: mitochondrial fissi. on 1; HSP60: heat shock protein 60; Mff: mitochondrial fission factor; PBM: photobiomodulation; SCI: spinal cord injury.

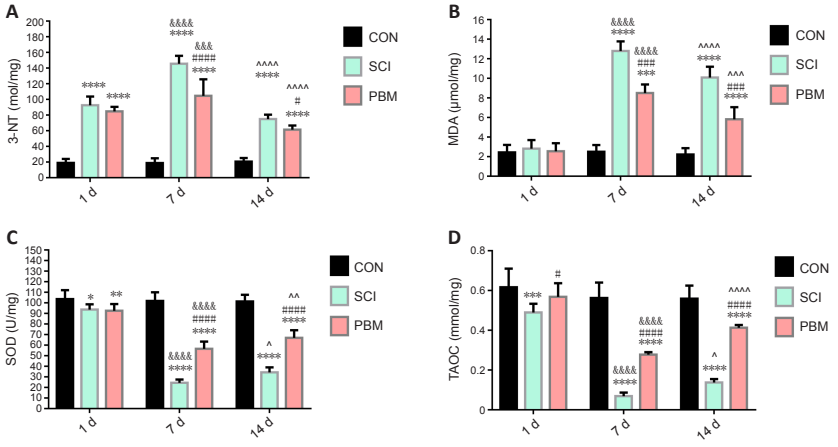

Figure 3 | **Effects of PBM on mitochondrial oxidative stress at 1, 7 and 14 days after SCI.**
(A, B) Quantitative analyses of oxidative stress markers specific to protein (3-NT, A) and lipid oxidation (MDA, B) in spinal cord tissue homogenates at 1, 7 and 14 days post-SCI. (C, D) Antioxidative parameters, namely SOD (C) and TAOC (D), were quantified in spinal cord tissue homogenates at 1, 7 and 14 days after SCI. Data are expressed as mean ± SEM (n = 6). *P < 0.05, **P < 0.01, ***P < 0.001, ****P < 0.0001, *vs.* CON group; ###P < 0.001, ####P < 0.0001, *vs.* SCI group; &&&&P < 0.0001, *vs.*1 day post-operation; ^P < 0.05, ^^P < 0.01, ^^^P < 0.001, ^^^^P < 0.0001, *vs.* 7 days post-operation (one-way analysis of variance followed by least significant difference *post hoc* test). 3-NT: 3-Nitrotyrosine; MDA: malondialdehyde; PBM: photobiomodulation; SCI: spinal cord injury; SOD: superoxide dismutase; TAOC: total antioxidant capacity.

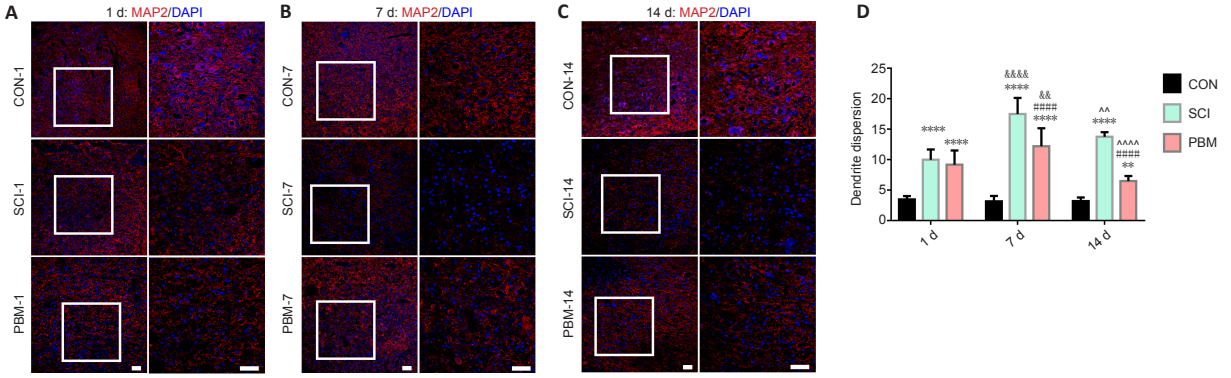

Figure 4 | **Effects of PBM on neuronal injury at 1, 7 and 14 days after SCI.**
(A–C) Representative MAP2 (red, Cy3) fluorescence images of neurons in ventral spinal cord from rats at 1 (A), 7 (B) and 14 (C) days post-SCI. Scale bars: 20 μm. (D) Quantitative analyses of MAP2 dispersion in ventral spinal cord at 1, 7 and 14 days after operation. Data are expressed as mean ± SEM (n = 5). $^{**}P < 0.01$, $^{****}P < 0.0001$, *vs*. CON group; $\#\#\#\#P < 0.0001$, *vs*, SCI group; $\&\&P < 0.01$, $\&\&\&\&P < 0.0001$, *vs*. 1 day post-operation; $\wedge\wedge P < 0.01$, *vs*. 7 days post-operation (one-way analysis of variance followed by least significant difference *post hoc* test). CON: Control; DAPI: 4′,6-diamidino-2-phenylindole; MAP2: microtubule-associated protein 2; PBM: photobiomodulation; SCI: spinal cord injury.

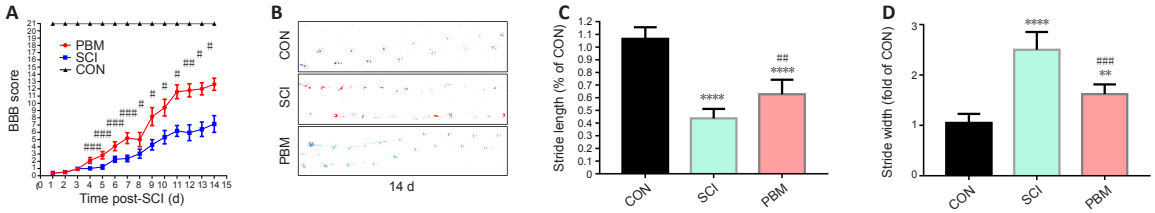

Figure 5 | **Effects of PBM on motor function recovery after SCI.**
(A, B) Locomotor function recovery was measured by BBB score and footprint analysis. SCI rats had impaired motor function, which gradually recovered over time. PBM had a time-dependent effect on promotion of motor function recovery. (C, D) Statistical analyses of stride length and stride width from footprint analysis at 14 days post-SCI. Data are expressed as mean ± SEM (n = 5). $^{**}P < 0.01$, $^{****}P < 0.0001$, *vs*. CON group; $\#P < 0.05$, $\#\#P < 0.01$, $\#\#\#P < 0.001$, *vs*. SCI group (one-way analysis of variance followed by least significant difference *post hoc* test). BBB: Basso, Beattie, and Bresnahan; CON: control; PBM: photobiomodulation; SCI: spinal cord injury.

It has been suggested that Drp1 drives abnormal mitochondrial fission through binding to the outer membrane adaptors Fis1 (Frank et al., 2001; Yu et al., 2013; Hu et al., 2017) and MFF (Otera et al., 2010; Otera and Mihara, 2011), which the aggravates mitochondrial dysfunction, such as energy depletion, oxidative stress, and cell apoptosis, and leads to the loss of function. Drp1-dependent mitochondrial fragmentation has been shown to promote delayed neuronal cell death according to the colocalization of proapoptotic proteins, such as Bax and Bcl-2 antagonist/killer (Arnoult et al., 2005; Karbowski et al., 2006; Montessuit et al., 2010; Landes and Martinou, 2011). In the present study, we demonstrated that the effects of PBM on mitochondrial-related fission proteins, oxidative stress, neuronal injury and locomotor function recovery varied with mitochondrial changes in number and morphology in the subacute phase. Thus, the findings suggest self-repair of the mitochondrial fission imbalance and that the treatment effect of PBM on mitochondrial fragmentation improved with time.

Swollen mitochondria were observed at 1 day after injury, indicating that the mechanical trauma induced immediate mitochondrial damage. PBM partly restored the swollen mitochondrial damage in the acute phase, but it did not improve oxidative stress and neuronal damage, or prevent the deterioration of oxidative stress and neuronal damage, suggesting that PBM could not prevent secondary damage from progressing via restoring the swollen mitochondria in the acute phase. Under physiological conditions, approximately 90% of reactive oxygen species are generated as by-products of mitochondrial metabolism. In the present study, protein oxidation was increased, but not lipid oxidation, suggesting that protein oxidation is a key target for SCI in the acute phase.

There are some limitations to the present study that need to be addressed. Assessment of the behavioral response in the present study was limited to motor function, though previous studies have reported that PBM is also effective against neuropathic pain (Micheli et al., 2017, 2019). The key molecular and signaling mechanisms of PBM in improving neuropathic pain remain unknown. Additionally, this study focused only on the subacute phase after SCI. It remains unknown whether continuous PBM treatment in the chronic phase after SCI would further promote functional recovery and whether the recovery would be maintained after the cessation of PBM therapy. The key molecular and signaling mechanisms of PBM in regulating mitochondrial fission imbalance remain unknown. The issues mentioned above need attention and further investigation.

In conclusion, our findings support that mitochondrial fission imbalance is related to secondary injury progression in the subacute phase of SCI and ultimately to neuronal apoptosis. The findings suggest that PBM provided an effective protective mechanism to prevent neuronal damage and dysfunction caused by mitochondrial fragmentation after SCI in the subacute phase. Thus, the present research suggests that PBM may be a potential and safe interventional strategy for SCI.

Author contributions: *Study conception and design: ZW, XL, XYH, XKW; experimental implementation: XL, ZJZ, XSZ, ZWL, TD, KL, XKW; data analysis: XL, ZJZ, YGM, PHL, CJ, ZHZ, ZWS, HLQ, JWZ, LL; manuscript draft: ZW, XL, XYH. All authors read and approved the final version of the manuscript.*
Conflicts of interest: *The authors declare no conflicts of interest.*
Data availability statement: *All relevant data are within the paper and its Additional files.*

Open peer reviewer: *Lorenzo Di Cesare Mannelli, University of Florence, Italy.*
Additional files:
Additional Figure 1: *Animal experimental design and PBM administration.*
Additional Figure 2: *Effects of PBM on mitochondrial morphology at 1 day after SCI.*
Additional Figure 3: *Effects of PBM on apoptosis at 14 days after SCI.*
Additional file 1: *Open peer review report 1.*

References

Arnoult D, Rismanchi N, Grodet A, Roberts RG, Seeburg DP, Estaquier J, Sheng M, Blackstone C (2005) Bax/Bak-dependent release of DDP/TIMM8a promotes Drp1-mediated mitochondrial fission and mitoptosis during programmed cell death. Curr Biol 15:2112-2118.

Bains M, Hall ED (2012) Antioxidant therapies in traumatic brain and spinal cord injury. Biochim Biophys Acta 1822:675-684.

Basso DM, Beattie MS, Bresnahan JC (1995) A sensitive and reliable locomotor rating scale for open field testing in rats. J Neurotrauma 12:1-21.

Calkins MJ, Manczak M, Mao P, Shirendeb U, Reddy PH (2011) Impaired mitochondrial biogenesis, defective axonal transport of mitochondria, abnormal mitochondrial dynamics and synaptic degeneration in a mouse model of Alzheimer's disease. Hum Mol Genet 20:4515-4529.

Cao Y, Lv G, Wang YS, Fan ZK, Bi YL, Zhao L, Guo ZP (2013) Mitochondrial fusion and fission after spinal sacord injury in rats. Brain Res 1522:59-66.

Cavalier-Smith T (2006) Origin of mitochondria by intracellular enslavement of a photosynthetic purple bacterium. Proc Biol Sci 273:1943-1952.

Chen X, Cui J, Zhai X, Zhang J, Gu Z, Zhi X, Weng W, Pan P, Cao L, Ji F, Wang Z, Su J (2018) Inhalation of hydrogen of different concentrations ameliorates spinal cord injury in mice by protecting spinal cord neurons from apoptosis, oxidative injury and mitochondrial structure damages. Cell Physiol Biochem 47:176-190.
de Medinaceli L, Freed WJ, Wyatt RJ (1982) An index of the functional condition of rat sciatic nerve based on measurements made from walking tracks. Exp Neurol 77:634-643.
Donovan J, Kirshblum S (2018) Clinical trials in traumatic spinal cord injury. Neurotherapeutics 15:654-668.
Eells JT, Wong-Riley MT, VerHoeve J, Henry M, Buchman EV, Kane MP, Gould LJ, Das R, Jett M, Hodgson BD, Margolis D, Whelan HT (2004) Mitochondrial signal transduction in accelerated wound and retinal healing by near-infrared light therapy. Mitochondrion 4:559-567.
Fatima G, Sharma VP, Das SK, Mahdi AA (2015) Oxidative stress and antioxidative parameters in patients with spinal cord injury: implications in the pathogenesis of disease. Spinal Cord 53:3-6.
Frank S, Gaume B, Bergmann-Leitner ES, Leitner WW, Robert EG, Catez F, Smith CL, Youle RJ (2001) The role of dynamin-related protein 1, a mediator of mitochondrial fission, in apoptosis. Dev Cell 1:515-525.
Gollihue JL, Rabchevsky AG (2017) Prospects for therapeutic mitochondrial transplantation. Mitochondrion 35:70-79.
Grohm J, Plesnila N, Culmsee C (2010) Bid mediates fission, membrane permeabilization and peri-nuclear accumulation of mitochondria as a prerequisite for oxidative neuronal cell death. Brain Behav Immun 24:831-838.
Grohm J, Kim SW, Mamrak U, Tobaben S, Cassidy-Stone A, Nunnari J, Plesnila N, Culmsee C (2012) Inhibition of Drp1 provides neuroprotection in vitro and in vivo. Cell Death Differ 19:1446-1458.
Guan Y, Chen C, Guo A, Wei J, Cai J, Han H, Hei Z, Tan H, Li X (2021) Prolonged symptom onset to admission time is associated with severe Coronavirus disease: A meta combined propensity-adjusted analysis. J Med Virol 93:6714-6721.
Hachem LD, Ahuja CS, Fehlings MG (2017) Assessment and management of acute spinal cord injury: from point of injury to rehabilitation. J Spinal Cord Med 40:665-675.
Hall ED (2011) Antioxidant therapies for acute spinal cord injury. Neurotherapeutics 8:152-167.
Hoppins S, Lackner L, Nunnari J (2007) The machines that divide and fuse mitochondria. Annu Rev Biochem 76:751-780.
Hu C, Huang Y, Li L (2017) Drp1-dependent mitochondrial fission plays critical roles in physiological and pathological progresses in mammals. Int J Mol Sci 18:144.
Huisa BN, Chen Y, Meyer BC, Tafreshi GM, Zivin JA (2013) Incremental treatments with laser therapy augments good behavioral outcome in the rabbit small clot embolic stroke model. Lasers Med Sci 28:1085-1089.
Jazayeri SB, Beygi S, Shokraneh F, Hagen EM, Rahimi-Movaghar V (2015) Incidence of traumatic spinal cord injury worldwide: a systematic review. Eur Spine J 24:905-918.
Jia ZQ, Li G, Zhang ZY, Li HT, Wang JQ, Fan ZK, Lv G (2016) Time representation of mitochondrial morphology and function after acute spinal cord injury. Neural Regen Res 11:137-143.
Karbowski M, Norris KL, Cleland MM, Jeong SY, Youle RJ (2006) Role of Bax and Bak in mitochondrial morphogenesis. Nature 443:658-662.
Karu T, Tiphlova O, Esenaliev R, Letokhov V (1994) Two different mechanisms of low-intensity laser photobiological effects on Escherichia coli. J Photochem Photobiol B 24:155-161.
Karu TI (2008) Mitochondrial signaling in mammalian cells activated by red and near-IR radiation. Photochem Photobiol 84:1091-1099.
Karu TI, Pyatibrat LV, Ryabykh TP (2003) Melatonin modulates the action of near infrared radiation on cell adhesion. J Pineal Res 34:167-172.
Karu TI, Pyatibrat LV, Kalendo GS (2004) Photobiological modulation of cell attachment via cytochrome c oxidase. Photochem Photobiol Sci 3:211-216.
Karu TI, Pyatibrat LV, Kolyakov SF, Afanasyeva NI (2005) Absorption measurements of a cell monolayer relevant to phototherapy: reduction of cytochrome c oxidase under near IR radiation. J Photochem Photobiol B 81:98-106.
Landes T, Martinou JC (2011) Mitochondrial outer membrane permeabilization during apoptosis: the role of mitochondrial fission. Biochim Biophys Acta 1813:540-545.
Li G, Jia Z, Cao Y, Wang Y, Li H, Zhang Z, Bi J, Lv G, Fan Z (2015) Mitochondrial division inhibitor 1 ameliorates mitochondrial injury, apoptosis, and motor dysfunction after acute spinal cord injury in rats. Neurochem Res 40:1379-1392.
Liang HL, Whelan HT, Eells JT, Meng H, Buchmann E, Lerch-Gaggl A, Wong-Riley M (2006) Photobiomodulation partially rescues visual cortical neurons from cyanide-induced apoptosis. Neuroscience 139:639-649.
Liang Z, Lei T, Wang S, Zuo X, Li K, Song J, Sun J, Zhang J, Zheng Q, Kang X, Ma Y, Hu X, Ding T, Wang Z (2020) Photobiomodulation by diffusing optical fiber on spinal cord: a feasibility study in piglet model. Journal of biophotonics 13:e201960022.
Liu JM, Yi Z, Liu SZ, Chang JH, Dang XB, Li QY, Zhang YL (2015) The mitochondrial division inhibitor mdivi-1 attenuates spinal cord ischemia-reperfusion injury both in vitro and in vivo: involvement of BK channels. Brain Res 1619:155-165.
Liu K, Zhao Q, Liu P, Cao J, Gong J, Wang C, Wang W, Li X, Sun H, Zhang C, Li Y, Jiang M, Zhu S, Sun Q, Jiao J, Hu B, Zhao X, Li W, Chen Q, Zhou Q, et al. (2016) ATG3-dependent autophagy mediates mitochondrial homeostasis in pluripotency acquirement and maintenance. Autophagy 12:2000-2008.
Lu Y, Wang R, Dong Y, Tucker D, Zhao N, Ahmed ME, Zhu L, Liu TC, Cohen RM, Zhang Q (2017) Low-level laser therapy for beta amyloid toxicity in rat hippocampus. Neurobiol Aging 49:165-182.
McEwen ML, Sullivan PG, Springer JE (2007) Pretreatment with the cyclosporin derivative, NIM811, improves the function of synaptic mitochondria following spinal cord contusion in rats. J Neurotrauma 24:613-624.
Meyer JN, Leuthner TC, Luz AL (2017) Mitochondrial fusion, fission, and mitochondrial toxicity. Toxicology 391:42-53.
Micheli L, Di Cesare Mannelli L, Lucarini E, Cialdai F, Vignali L, Ghelardini C, Monici M (2017) Photobiomodulation therapy by NIR laser in persistent pain: an analytical study in the rat. Lasers Med Sci 32:1835-1846.
Micheli L, Cialdai F, Pacini A, Branca JJV, Morbidelli L, Ciccone V, Lucarini E, Ghelardini C, Monici M, Di Cesare Mannelli L (2019) Effect of NIR laser therapy by MLS-MiS source against neuropathic pain in rats: in vivo and ex vivo analysis. Sci Rep 9:9297.
Montessuit S, Somasekharan SP, Terrones O, Lucken-Ardjomande S, Herzig S, Schwarzenbacher R, Manstein DJ, Bossy-Wetzel E, Basañez G, Meda P, Martinou JC (2010) Membrane remodeling induced by the dynamin-related protein Drp1 stimulates Bax oligomerization. Cell 142:889-901.
Morimoto Y, Arai T, Kikuchi M, Nakajima S, Nakamura H (1994) Effect of low-intensity argon laser irradiation on mitochondrial respiration. Lasers Surg Med 15:191-199.
Otera H, Mihara K (2011) Discovery of the membrane receptor for mitochondrial fission GTPase Drp1. Small GTPases 2:167-172.
Otera H, Wang C, Cleland MM, Setoguchi K, Yokota S, Youle RJ, Mihara K (2010) Mff is an essential factor for mitochondrial recruitment of Drp1 during mitochondrial fission in mammalian cells. J Cell Biol 191:1141-1158.
Ottolini D, Calí T, Szabò I, Brini M (2017) Alpha-synuclein at the intracellular and the extracellular side: functional and dysfunctional implications. Biol Chem 398:77-100.
Ozgen S, Krigman J, Zhang R, Sun N (2022) Significance of mitochondrial activity in neurogenesis and neurodegenerative diseases. Neural Regen Res 17:741-747.
Pastore D, Greco M, Passarella S (2000) Specific helium-neon laser sensitivity of the purified cytochrome c oxidase. Int J Radiat Biol 76:863-870.
Patel SP, Sullivan PG, Lyttle TS, Rabchevsky AG (2010) Acetyl-L-carnitine ameliorates mitochondrial dysfunction following contusion spinal cord injury. J Neurochem 114:291-301.
Percie du Sert N, Hurst V, Ahluwalia A, Alam S, Avey MT, Baker M, Browne WJ, Clark A, Cuthill IC, Dirnagl U, Emerson M, Garner P, Holgate ST, Howells DW, Karp NA, Lazic SE, Lidster K, MacCallum CJ, Macleod M, Pearl EJ, et al. (2020) The ARRIVE guidelines 2.0: Updated guidelines for reporting animal research. PLoS Biol 18:e3000410.
Qiao F, Atkinson C, Kindy MS, Shunmugavel A, Morgan BP, Song H, Tomlinson S (2010) The alternative and terminal pathways of complement mediate post-traumatic spinal cord inflammation and injury. Am J Pathol 177:3061-3070.
Qiao H, Zhang Q, Yuan H, Li Y, Wang D, Wang R, He X (2015) Elevated neuronal α-synuclein promotes microglia activation after spinal cord ischemic/reperfused injury. Neuroreport 26:656-661.
Ravikumar R, McEwen ML, Springer JE (2007) Post-treatment with the cyclosporin derivative, NIM811, reduced indices of cell death and increased the volume of spared tissue in the acute period following spinal cord contusion. J Neurotrauma 24:1618-1630.
Rey F, Ottolenghi S, Zuccotti GV, Samaja M, Carelli S (2022) Mitochondrial dysfunctions in neurodegenerative diseases: role in disease pathogenesis, strategies for analysis and therapeutic prospects. Neural Regen Res 17:754-758.
Schindelin J, Arganda-Carreras I, Frise E, Kaynig V, Longair M, Pietzsch T, Preibisch S, Rueden C, Saalfeld S, Schmid B, Tinevez JY, White DJ, Hartenstein V, Eliceiri K, Tomancak P, Cardona A (2012) Fiji: an open-source platform for biological-image analysis. Nat Methods 9:676-682.
Scholpa NE, Schnellmann RG (2017) Mitochondrial-based therapeutics for the treatment of spinal cord injury: mitochondrial biogenesis as a potential pharmacological target. J Pharmacol Exp Ther 363:303-313.
Song JW, Li K, Liang ZW, Dai C, Shen XF, Gong YZ, Wang S, Hu XY, Wang Z (2017) Low-level laser facilitates alternatively activated macrophage/microglia polarization and promotes functional recovery after crush spinal cord injury in rats. Sci Rep 7:620.
Suárez-Rivero JM, Villanueva-Paz M, de la Cruz-Ojeda P, de la Mata M, Cotán D, Oropesa-Ávila M, de Lavera I, Álvarez-Córdoba M, Luzón-Hidalgo R, Sánchez-Alcázar JA (2016) Mitochondrial dynamics in mitochondrial diseases. Diseases 5:1.
Tait SW, Green DR (2012) Mitochondria and cell signalling. J Cell Sci 125:807-815.
Vacca RA, Marra E, Quagliariello E, Greco M (1993) Activation of mitochondrial DNA replication by He-Ne laser irradiation. Biochem Biophys Res Commun 195:704-709.
Wang X, Li X, Zuo X, Liang Z, Ding T, Li K, Ma Y, Li P, Zhu Z, Ju C, Zhang Z, Song Z, Quan H, Zhang J, Hu X, Wang Z (2021) Photobiomodulation inhibits the activation of neurotoxic microglia and astrocytes by inhibiting Lcn2/JAK2-STAT3 crosstalk after spinal cord injury in male rats. J Neuroinflammation 18:256.
Xuan W, Vatansever F, Huang L, Hamblin MR (2014) Transcranial low-level laser therapy enhances learning, memory, and neuroprogenitor cells after traumatic brain injury in mice. J Biomed Opt 19:108003.
Yeager RL, Franzosa JA, Millsap DS, Lim J, Heise SS, Wakhungu P, Whelan HT, Eells JT, Henshel DS (2006) Survivorship and mortality implications of developmental 670-nm phototherapy: dioxin co-exposure. Photomed Laser Surg 24:29-32.
Ying R, Liang HL, Whelan HT, Eells JT, Wong-Riley MT (2008) Pretreatment with near-infrared light via light-emitting diode provides added benefit against rotenone- and MPP+-induced neurotoxicity. Brain Res 1243:167-173.
Youle RJ, van der Bliek AM (2012) Mitochondrial fission, fusion, and stress. Science 337:1062-1065.
Yu D, Li M, Ni B, Kong J, Zhang Z (2013) Induction of neuronal mitophagy in acute spinal cord injury in rats. Neurotox Res 24:512-522.
Zhang LJ, Chen Y, Wang LX, Zhuang XQ, Xia HC (2021) Identification of potential oxidative stress biomarkers for spinal cord injury in erythrocytes using mass spectrometry. Neural Regen Res 16:1294-1301.

P-Reviewer: Di Cesare Mannelli L; C-Editor: Zhao M; S-Editors: Yu J, Li CH;
L-Editors: McCollum L, Yu J, Song LP; T-Editor: Jia Y